Cell Reports, Volume *31*

Supplemental Information

Antagonistic Center-Surround Mechanisms for Direction Selectivity in the Retina

Lea Ankri, Elishai Ezra-Tsur, Shir R. Maimon, Nathali Kaushansky, and Michal Rivlin-Etzion

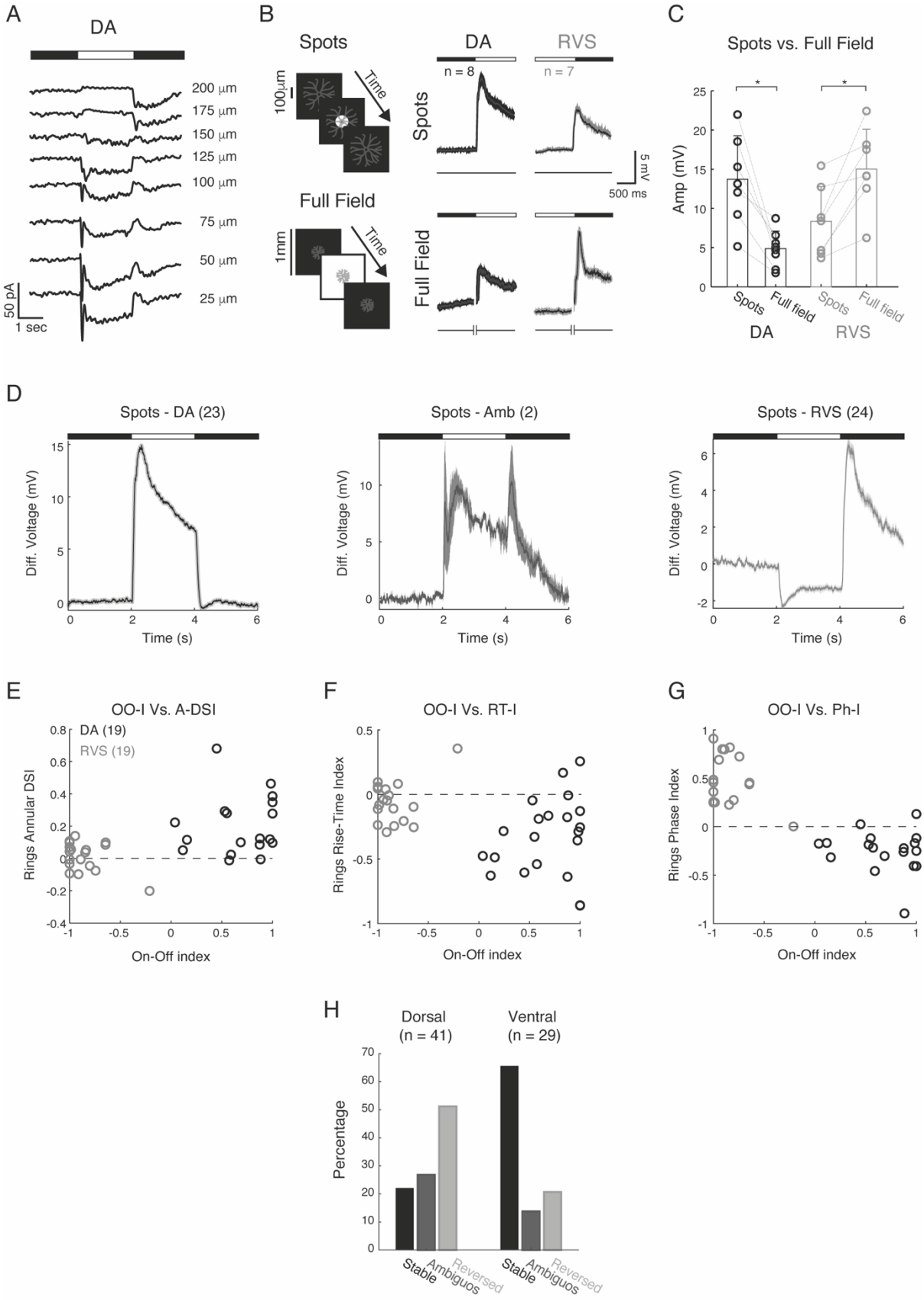
A
DA
200 µm
175 µm
150 µm
125 µm
100 µm
75 µm
50 µm
25 µm
50 pA
1 sec
B
Spots
100µm
Time
Full Field
1mm
Time
DA
RVS
n = 8
n = 7
Spots
Full Field
5 mV
500 ms
C
Spots vs. Full Field
Amp (mV)
Spots
Full field
Spots
Full field
DA
RVS
D
Spots - DA (23)
Spots - Amb (2)
Spots - RVS (24)
Diff. Voltage (mV)
Time (s)
E
OO-I Vs. A-DSI
DA (19)
RVS (19)
Rings Annular DSI
On-Off index
F
OO-I Vs. RT-I
Rings Rise-Time Index
On-Off index
G
OO-I Vs. Ph-I
Rings Phase Index
On-Off index
H
Dorsal
(n = 41)
Ventral
(n = 29)
Percentage
Stable
Ambiguos
Reversed

Figure S1: Characterizing On-SAC responses in dark adapted conditions and following RVS. Related to Figures 1 and 2.

(A) Excitatory inputs (holding voltage = -60 mV) to an example DA SAC in response to presentation of bright rings in different radii (8 rings, radii are denoted on right; see Figure 1D). In response to the smaller rings On excitation was prominent, whereas larger rings elicited Off surround activation. This surround activation was present in a portion of DA-SAC (see example of a DA SAC that did nor display surround activation in main Figure 1D).

(B) *Left*: illustration of the stimuli. On-SACs were presented with a bright spot of 100 μm diameter (top) and a full field illumination (bottom, covering 1 mm diameter). *Right*: On-SAC voltage responses (Mean ± SEM) to spots (top) and full field illumination (bottom), in DA conditions (black, left) and following RVS (grey, right). For DA SACs responses emerged to the bright stimulus, whereas responses emerged to its disappearance following RVS (The discontinuity in the full-field response is due to the recording protocol: SAC baseline was taken from the end of the recordings). n denotes number of cells.

(C) Comparison of the voltage amplitudes in response to spots and full field illumination, in DA conditions and following RVS. In DA conditions On-SACs response amplitude to spots stimulation was larger than their response to full field illumination, and this relationship reversed following RVS (*$p < 0.05$; student's t-test).

(D) Current clamp recordings (Mean ± SEM; baseline set to 0) in response to a spot stimulus of all DA On-SAC that displayed pure On response (23/25; left), On-SAC that displayed ambiguous response (-0.1 < On-Off-index < 0.1; 2/25, middle), and all On-SAC that displayed Off response following RVS (24/25, right; One On-SAC displayed a stable On response following RVS and was discarded from further analysis).

(E) On-Off index (OOI) vs. rings annular DSI of On-SAC that were stimulated by both spots and rings, in DA conditions and following RVS. Positive OOI values indicate stronger On response whereas negative values indicate stronger Off response; positive A-DSI values indicate stronger response to CF than CP motion.

(F) same as (E) but for rise-time index (see *Methods*). Negative RT-I values indicate shorter rise time in response to CF than to CP motion.

(G) same as (E) but for the response phase index. Negative Ph-I values indicate that response phase to CF motion arise earlier than response phase to CP motion.

(H) Percentage of stable, ambiguous and reversed DSGCs in the dorsal (left) and ventral (right) retina following RVS. This plot is based on published data (Rivlin-Etzion et al., 2012) after separating DSGCs recorded in dorsal and ventral retina.

The opposed relationship between the responses to the spot stimulus and the full field stimulus (B, C) indicates that SAC receptive field has expanded. This is in accordance with the shift in location of SAC activation from proximal (in DA conditions) to distal (following RVS) receptive field (Figure 2F).

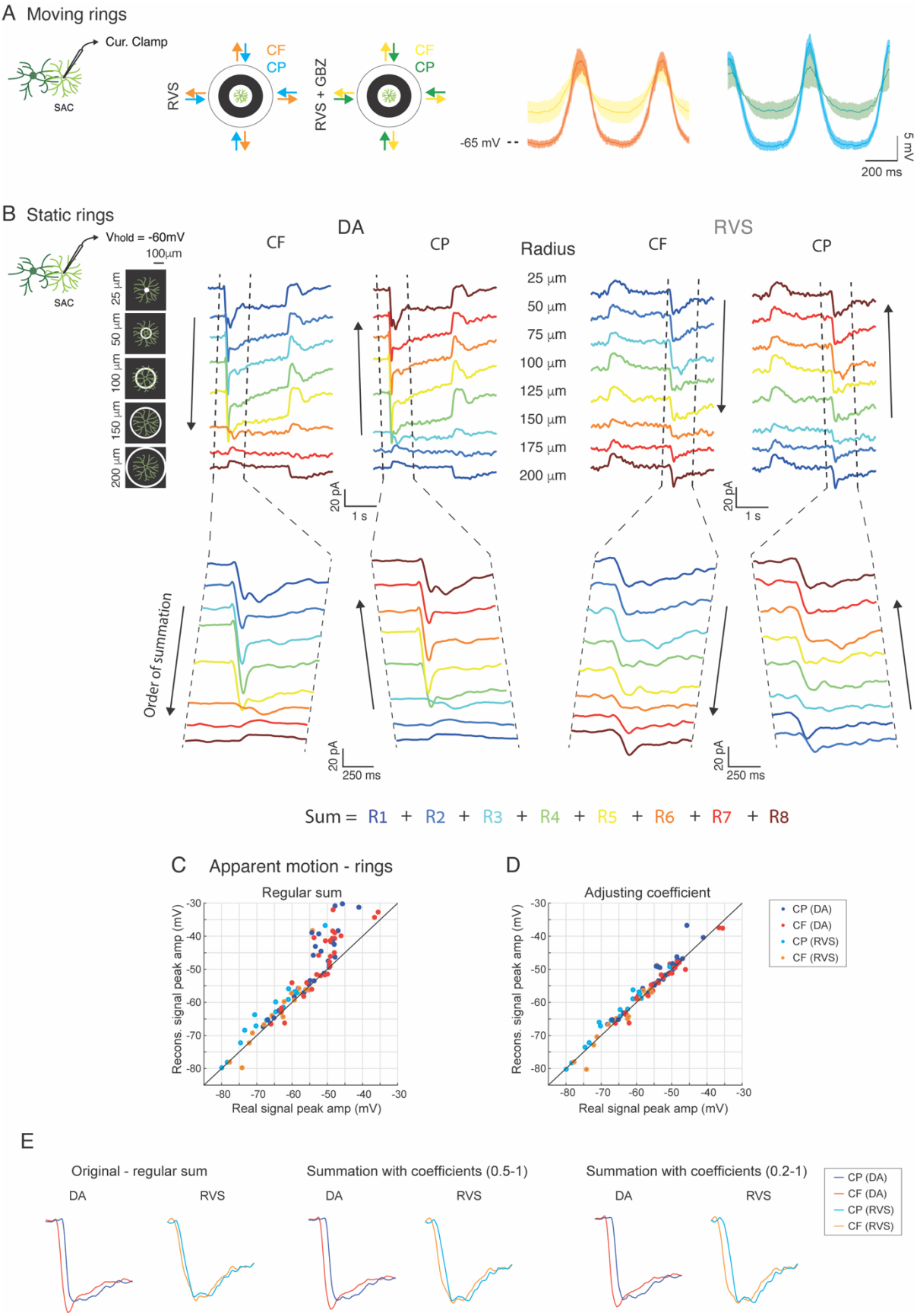

Figure S2. Linear spatiotemporal model of SAC directional responses. Related to Figures 2 and 3.

(A) *Left:* Illustration of CF and CP motion presented to On-SAC following RVS and after application of GABA-A blocker. *Right:* 1 second average current clamp recordings from On-SACs (Mean ± SEM) in response to CF and CP rings presentation, following RVS and after addition of GABA-A blocker (SR95531; 10 μM; n=4 cells). GABA-A receptors blockade does not change the phase of the response but abolishes the hyperpolarizing response to the bright ring.

(B) Population average of EPSCs (Vhold = -60 mV) evoked in DA (left) and RVS SACs (right) in response to 8 rings of different radii (5 of which are illustrated on the left; all rings radii are marked in the middle). The traces are color coded by their time shift, where the blue trace is not shifted and each consecutive trace in shifted in time by 27 ms from its previous (with last trace shown in brown shifted by 7x27 ms = 189 ms). CF motion simulation is depicted on left and CP motion simulation is depicted on right. Tilted vertical lines indicate the time window used for linear summation of the responses. *Bottom*: magnification of the time window used for linear summation in (E) and in Figure 3A, B.

(C-E) Validation of the model: the model assumes linear summation, but SACs may perform nonlinear signal integration (Euler et al., 2002; Gavrikov et al., 2006; Hausselt et al., 2007; Oesch and Taylor, 2010; Ozaita et al., 2004). We therefore presented On-SACs with two static rings of different radii (ranging from 50-280 μm), presented either in isolation or sequentially to mimic CF or CP motion (apparent motion). We then validated the model by comparing voltage responses during apparent motion to the reconstructed motion response based on linear summation of the responses to the two static rings. This comparison shows that linear summation in most SACs resembles their response to apparent motion (C). Adjusting coefficients to the big ring in the linear summation minimized distance between peak response amplitude in apparent motion and the reconstructed signal (D). Adding coefficients did not qualitatively change the results (E). *Left:* the resulting linear summation of the SAC responses in DA conditions and following RVS to CF- and CP-like motion (as in Figure 3A, B); *Middle:* linear summation when using coefficients for the big ring, determined by ring size and decreasing from 1 to 0.5 with ring radius; *Right*: linear summation when using coefficients which decrease from 1 to 0.2 with ring radius (right).

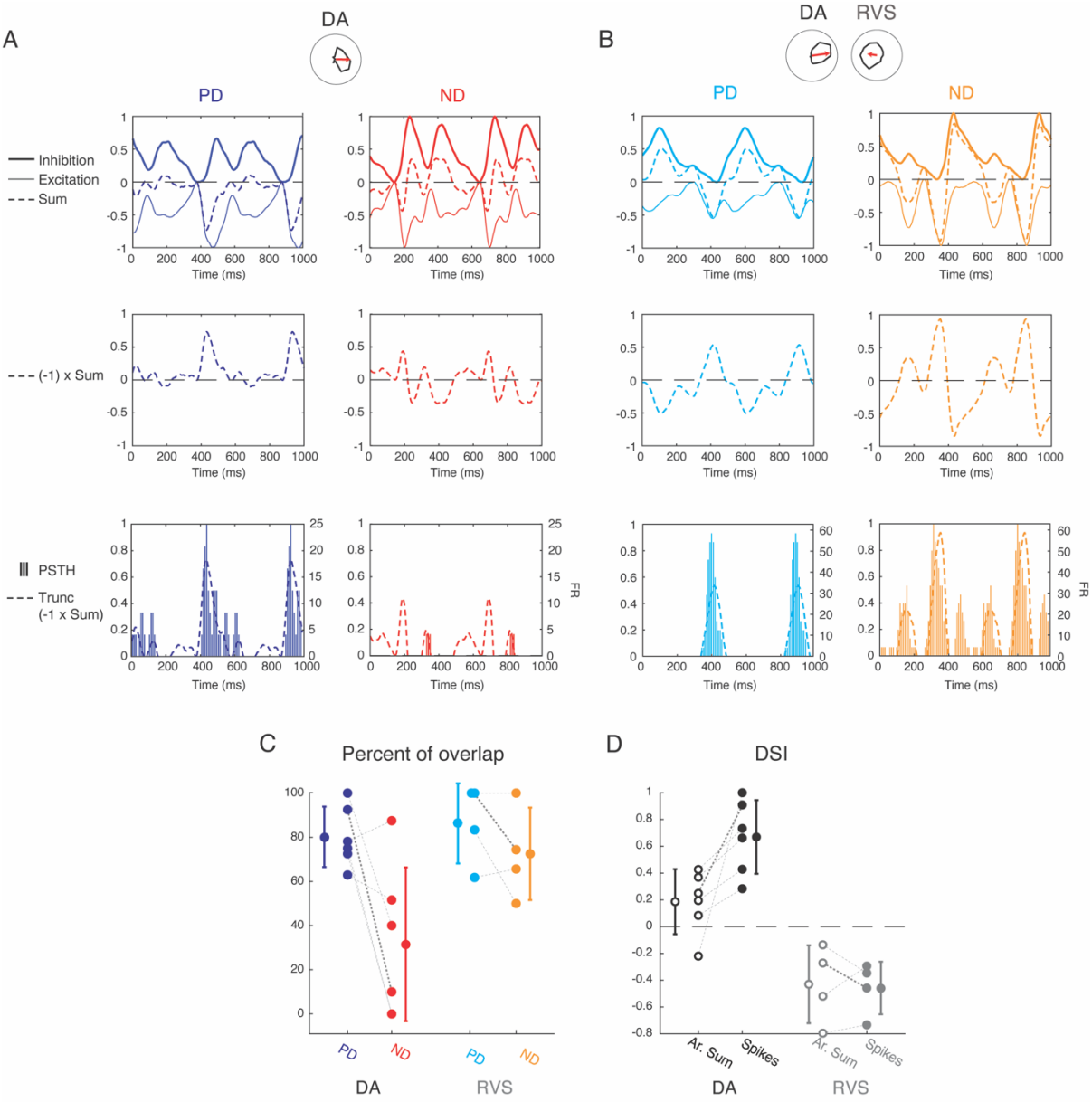

Figure S3. DSGCs spiking responses and synaptic inputs are correlated. Related to Figure 4.
(A) *Top*: normalized voltage clamp recordings (continuous lines, inhibition in bold) in the preferred (PD, blue; left) and null (ND, red, right) directions, recorded from an example DSGC (whose polar plot of spiking activity shown on top). The arithmetic summation of the normalized inhibition and excitation is superimposed (dashed line). *Middle*: the arithmetic summation is plotted reversed, to match the polarity of excitation to that of the PSTH – positive values correspond to stronger excitation. *Bottom*: the positive values of the arithmetic summation (truncated above 0) superimposed with the PSTH of spikes occurring in response to motion in either the preferred or null directions. Y axis on the right depicts the PSTH values (spikes/s, bin size=10 ms).
(B) Same as (A) but for a DSGC that reversed its directional tuning following RVS. The polar plot of the cell in DA conditions and following RVS is shown on top.
(C) Percent of overlap between the PSTH and the truncated arithmetic summation. Overlap tends to be ~80%, but is reduced in response to ND motion, probably due to the low firing rate that is often close to 0. Since following RVS the firing rate in response to PD motion is not as low, the overlap is higher.
(D) Comparison of the DSI of all cells in which both the spiking activity and the current responses to gratings stimulation were recorded. In DA conditions, 5/6 DSGCs displayed positive DSI in response to gratings both when calculated by the maximal value of the arithmetic summation and by the spiking activity. Following RVS, all 4 recorded cells displayed negative DSIs.

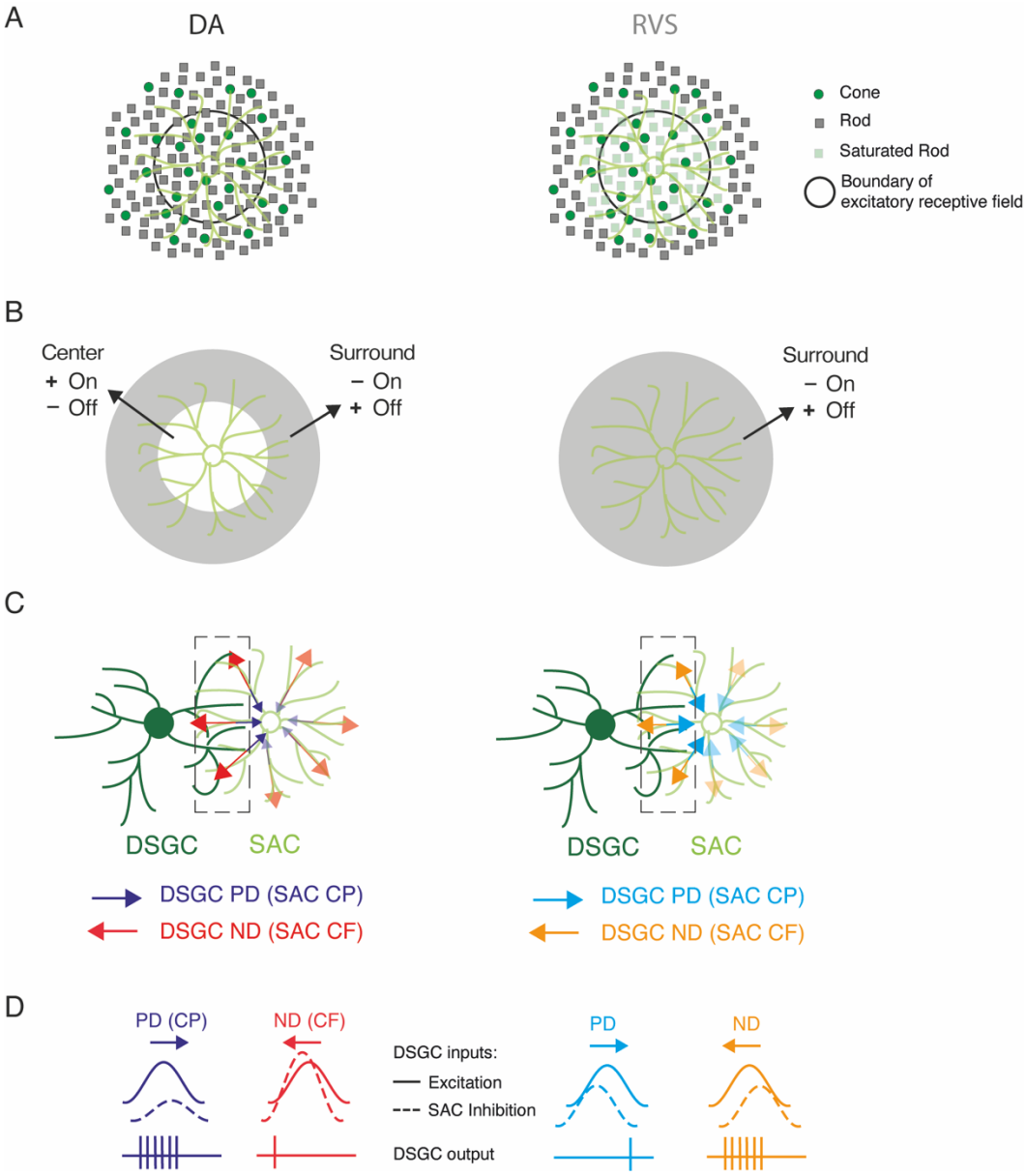

Figure S4: Summary of the changes in the direction selective circuit following RVS. Related to Figure 4.
(A) Excitatory inputs to SACs are restricted to the inner 2/3 of the dendritic arbor. In DA conditions (left), rods and cones depolarize to light offset. Following RVS (right), rods are saturated in the stimulated area and start serving as relay cells for cone-driven surround inhibition via horizontal cells (Vlasits et al., 2014).
(B) In DA conditions (left), both rods and cones mediate the On response in the center. Surround antagonism is primarily mediated by SAC inhibitory network. Off surround activation may result from disinhibition: inhibitory input from wide field amacrine cells to On bipolar cell terminals is relieved at light offset, leading to glutamate release (Lee and Zhou, 2006). Following RVS (right), saturated rods exhibit the opposite polarity response to light due to surround inhibition from cones, resulting in the loss of On response and expansion of the Off response (Vlasits et al., 2014).
(C) In DA conditions (left), center-surround organization supports SAC CF preference. Following RVS (right), loss of center-surround organization leads to loss of SAC CF preference, resulting in similar responses to CF and CP motion, which correspond to ND and PD motion in the DSGC they innervate, respectively. Dashed box denotes SAC processes that innervate the DSGC.
(D) Schematics of the excitatory-inhibitory balance in DSGCs: In DA conditions, the CF preference of SAC results in larger and faster inhibition to the DSGC during ND motion, which prevents firing. Following RVS, inhibition is no longer stronger during ND motion. Instead, inhibition arrives earlier during PD motion, due to changes in SAC receptive field organization, preventing firing during original PD motion. In response to ND motion, SAC inhibition arrives in delay, leading to reversal of DSGCs' directional preference.